Experimental Methods for Determining Aerodynamic Stability Derivatives of an Airplane in Wind Tunnels

By

Hiroshi MAEDA*

(Received April 30, 1960)

Two methods for determining the aerodynamic stability derivatives of an airplane in wind tunnels are investigated.

The principles of measurement are as follows:

(1) Determining the stability derivatives from the frequency response characteristics of a second order dynamic system with application of a forced oscillation of constant amplitude;

(2) Determining the stability derivatives from the transient response data of the model to a step control deflection input.

The former is suitable for low speed wind tunnel tests, and the latter is mainly for high speed wind tunnel tests.

In this paper the theoretical calculation and the preliminary experimental results are reported.

I. Introduction

In recent years, methods for determining the aerodynamic stability derivatives of an airplane in flight tests have made rapid progress and many reports have been published about the results of the work. However, it seems that the experimental methods in wind tunnels employing the model of an airplane for measuring the stability derivatives have not made remarkable development.

The author has investigated the usual methods for measuring the stability derivatives in wind tunnels, and originated suitable methods for both low and high speed wind tunnel tests with application of the principle of measurement in recent flight tests. By means of theoretical analysis and experimental research the following two methods have been established. The principles of measurement for these two methods are as follows:

(1) Determining the stability derivatives from the frequency response characteristics of a second order system by applying a steady forced oscillation with constant amplitude to the model;

* Department of Aeronautical Engineering

(2) Determining the stability derivatives from the transient response data of the model to a step control deflection.

The former is suitable for low speed wind tunnel tests principally, and it is supposed to involve the most desirable principles of measurement. On the other hand, the latter is a suitable mothod for high speed wind tunnels, in particular for tunnels of the intermittent type.

II. Forced Oscillation Method with Constant Amplitude

As is generally known, the forced oscillation method is the most desirable when the stability derivatives of an airplane model are measured in a wind tunnel. But the forced oscillation methods usually used in the past had many weak points in their principles or accuracies of measurement. Therefore, in order to overcome these disadvantages, the following experimental method has been devised. This method is at first sight similar to the well-known "Inexorable Forcing Method", but in principle of measurement it is rather similar to the usual forced oscillation method.

A. Principle of Measurement

(1) Measurement of Damping Derivatives and Stiffness Derivatives.

When a model is supported to rotate freely in the wind tunnel airstream about one axis, which is chosen at the design c.g. position, as shown in Fig. 1, Fig. 2 and Fig. 3, the equations of motion in each system are expressed as follows:

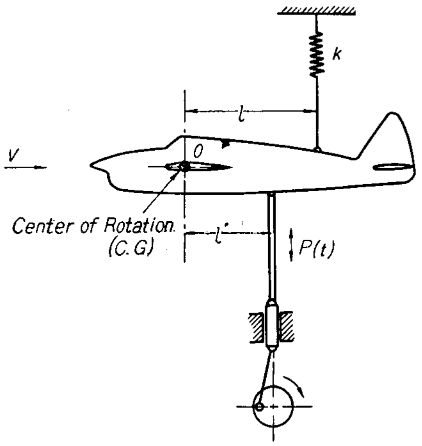

Fig. 1. Forced oscillation method. (pitching system)

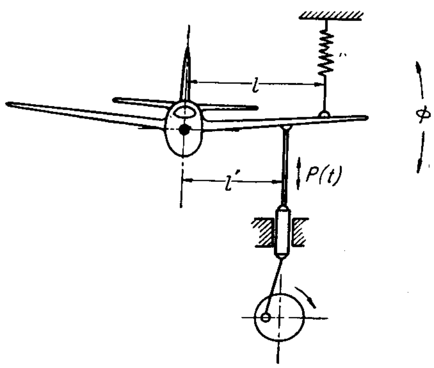

Fig. 2. Forced oscillation method. (rolling system)

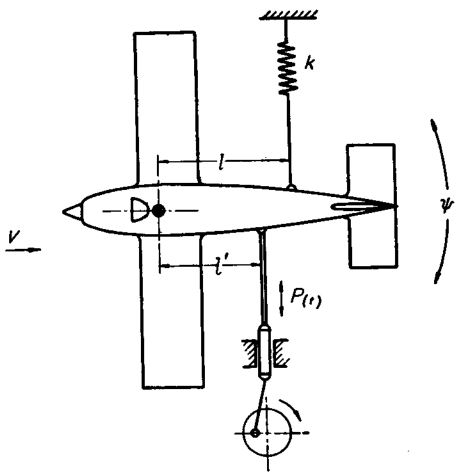

Fig. 3. Forced oscillation method. (yawing system)

$$B\ddot{\theta}+(-M_{\dot{\theta}})\dot{\theta}+(kl^2-M_\theta)\theta = M(t) \qquad (1)$$

$$M_{\dot{\theta}} = M_q+M_{\dot{\alpha}}$$

$$A\ddot{\phi}+(-L_p)\dot{\phi}+kl^2\phi = L(t) \qquad (2)$$

$$C\ddot{\psi}+(-Nr)\dot{\psi}+(kl^2-N_\psi)\psi = N(t)\,. \qquad (3)$$

Eq. (1), (2) and (3) are cases in the pitching, rolling and yawing systems, respectively. In the above equations $M(t)$, $L(t)$ and $N(t)$ are the applied forcing moment terms, and in this experimental method they are all equal to $P(t)\cdot l'$. Moreover, it is obvious that in these systems output angular displacement amplitudes are all constant regardless of the forcing frequency.

Eq. (1), (2) and (3) are all rewritten by the following simple equation

$$\ddot{x}+2\zeta\omega_n\dot{x}+\omega_n^2x = f(t) \qquad (4)$$

hence, if the input $f(t)$ is expressed by the following equation

$$f(t) = F\cdot\sin\omega t \qquad (5)$$

or $f(t)$ varies sinusoidally with amplitude F and circular frequency ω, the variations of amplitude and phase angle of output x are expressed by the frequency transfer function $G(j\omega)$ as follows;

$$G(j\omega) = \frac{1}{\omega_n^2}\cdot\frac{1}{\left\{1-\left(\frac{\omega}{\omega_n}\right)^2\right\}+2j\zeta\frac{\omega}{\omega_n}} \qquad (6)$$

$$= K\cdot M\cdot e^{i\varphi}\,. \qquad (6)'$$

By the absolute value and argument of Eq. (6), the amplitude ratio M, static gain K and phase angle φ are expressed by the following equations

$$M = \left[\left\{1-\left(\frac{\omega}{\omega_n}\right)^2\right\}^2+4\zeta^2\left(\frac{\omega}{\omega_n}\right)^2\right]^{-\frac{1}{2}} \qquad (7)$$

$$K = \frac{1}{\omega_n^2} \qquad (8)$$

$$\varphi = \tan^{-1}\frac{-2\zeta\frac{\omega}{\omega_n}}{1-\left(\frac{\omega}{\omega_n}\right)^2}\,. \qquad (9)$$

The graphical representation of the variations of M and φ against the damping ratio ζ and the frequency ω are shown in Fig. 4 and Fig. 5.

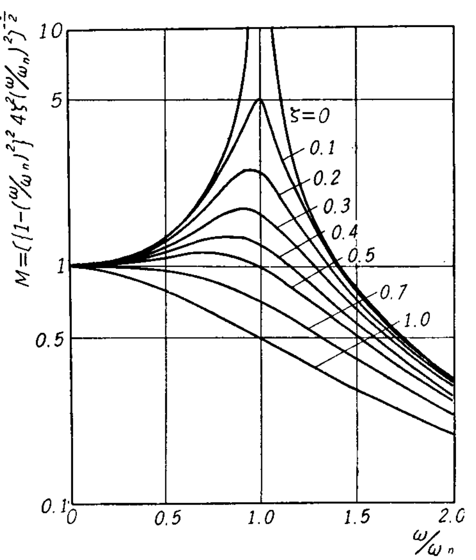

Fig. 4. Amplitude ratio diagram in second order system.

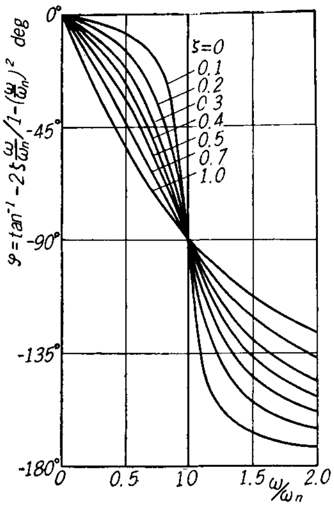

Fig. 5. Phase angle diagram in second order system.

Nevertheless, in this experimental method, the model makes steady oscillation with constant amplidude regardless of the values of ω and ζ as has been stated already, therefore

$$|x_s| = F\cdot K\cdot M = \frac{F}{\omega_n^2}\left[\left\{1-\left(\frac{\omega}{\omega_n}\right)^2\right\}^2+4\zeta^2\left(\frac{\omega}{\omega_n}\right)^2\right]^{-\frac{1}{2}} = \text{const.} \tag{10}$$

where $|x_s|$ is the amplitude of x in steady oscillation. Hence

$$F = F_0\left[\left\{1-\left(\frac{\omega}{\omega_n}\right)^2\right\}^2+4\zeta^2\left(\frac{\omega}{\omega_n}\right)^2\right]^{\frac{1}{2}} \tag{11}$$

$$F_0 = |x_s|\cdot\omega_n^2 \tag{12}$$

where F_0 corresponds to the forcing moment which is necessary to give a constant displacement $|x_s|$ statically to the model. Therefore, if the amplitude ratio of the forcing moment is expressed by M',

$$M' = \frac{F}{F_0} = \left[\left\{1-\left(\frac{\omega}{\omega_n}\right)^2\right\}^2+4\zeta^2\left(\frac{\omega}{\omega_n}\right)^2\right]^{\frac{1}{2}} \tag{13}$$

hence M' is equal to the inverse of M. The variation of M' against ω and ζ is illustrated in Fig. 6.

The phenomenon shown in Fig. 6 may be understood in the following manners. In general forced oscillation, it is a well-known fact that, if the forcing input is given with constant amplitude, the output amplitude may increase at a frequency near the resonance point; and in particular, if the damping of the system is zero, the amplitude will be infinitely large theoretically at the resonance point. On the contrary, in this experimental method, since the output amplitude is always kept at a finite constant value, the forcing input amplitude will decrease inversely near the resonance point in general, and in the case of the zero damping, it will become zero at the resonance point.

Therefore, in the above mentioned experimental method, if the variation of the output or the model motion and the input or the forcing moment against the forcing frequencies are measured, it means that the frequency response of the second order system is determined, which can be seen from Eq. (7), (8) and (13).

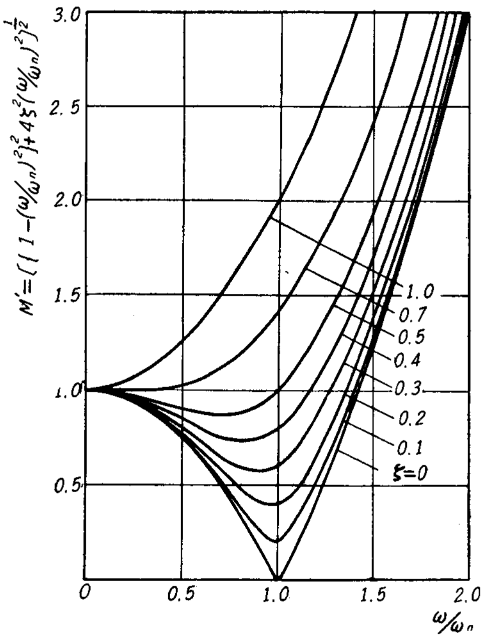

Fig. 6. Amplitude ratio of forcing moment.

With application of these frequency response characteristics, i.e. the amplitude ratio M and the phase angle φ, the stability derivatives in each system may be calculated by the following treatments. Using Eq. (7) and (8)

$$M=\frac{1}{\left[\left\{1-\left(\frac{\omega}{\omega_n}\right)^2\right\}^2(1+\tan^2\varphi)\right]^{\frac{1}{2}}}=\frac{|\cos\varphi|}{\left|1-\left(\frac{\omega}{\omega_n}\right)^2\right|}\,.$$

In the above equation, since $\cos\varphi$ and $1-\left(\frac{\omega}{\omega_n}\right)^2$ have always the same sign, it is possible to remove the sign of absolute value. Therefore

$$M=\frac{\cos\varphi}{1-\left(\frac{\omega}{\omega_n}\right)^2} \tag{14}$$

hence

$$\omega_n^2=\frac{\omega^2}{1-\frac{1}{M}\cos\varphi}=\frac{\omega^2}{1-M'\cos\varphi} \tag{15}$$

$$2\zeta\omega_n=\frac{\omega_n^2\cdot\sin\varphi}{M\cdot\omega}=M'\sin\varphi\frac{\omega_n^2}{\omega}\,. \tag{16}$$

Since ω_n^2 and $2\zeta\omega_n$ are the linear functions of the stability derivatives in each system, which can be seen from Eq. (1), (2) and (3), they are calculated as follows. In the case of the pitching system, using Eq. (1)

$$2\zeta\omega_n = -M_{\dot\theta}/B \tag{17}$$

$$\omega_n^2 = \frac{kl^2 - M_\theta}{B}\,. \tag{18}$$

Therefore, the stability derivatives $M_{\dot\theta}$ and M_θ are determined as follows;

$$M_{\dot\theta} = -B(2\zeta\omega_n) \tag{19}$$

$$M_\theta = kl^2 - B(\omega_n^2)\,. \tag{20}$$

In Eq. (19) and (20), the moment of inertia B, spring constant k and lever length l are all known quantities. Therefore, if ω_n^2 and $2\zeta\omega_n$ are determined from frequency response characteristics, the stability derivatives $M_{\dot\theta}$ and M_θ can be calculated using the above relations. These dimensional derivatives can be expressed in the following non-dimensional coefficient forms.

$$C_{m\dot\theta} = \frac{\partial C_m}{\partial\left(\frac{\dot\theta c}{2V}\right)} = \frac{M_{\dot\theta}}{\rho VS\left(\frac{c}{2}\right)^2} \tag{19$'$}$$

$$C_{m\dot\theta} = C_{mq} + C_{m\dot\alpha}$$

$$C_{m\theta} = \frac{\partial C_m}{\partial\theta} = \frac{M_\theta}{\rho V^2 S\left(\frac{c}{2}\right)}\,. \tag{20$'$}$$

In rolling and yawing system too, the stability derivatives L_p, N_r and N_ψ are similarly determined as follows:

$$L_p = -A(2\zeta\omega_n) \tag{21}$$

$$N_r = -C(2\zeta\omega_n) \tag{22}$$

$$N_\psi = kl^2 - C(\omega_n^2)\,. \tag{23}$$

These derivatives are also expressed in the non-dimensional coefficient form as follows:

$$C_{lp} = \frac{\partial C_l}{\partial\left(\frac{pb}{2V}\right)} = \frac{L_p}{\rho VS\left(\frac{b}{2}\right)^2} \tag{21$'$}$$

$$C_{nr} = \frac{\partial C_n}{\partial\left(\frac{rb}{2V}\right)} = \frac{N_r}{\rho VS\left(\frac{b}{2}\right)^2} \tag{22$'$}$$

$$C_{n\psi} = \frac{\partial C_n}{\partial\psi} = \frac{N_\psi}{\rho V^2 S\left(\frac{b}{2}\right)}\,. \tag{23$'$}$$

Moreover, in the case of the determination of damping derivatives $M_{\dot\theta}$, L_p and N_r, it is necessary to correct the mechanical damping effect which is contained in the damping term $2\zeta\omega_n$.

(2) Measurement of Cross Derivatives.

Independently of the measurement of L_p and N_r above mentioned, the cross derivatives N_p and L_r can be determined by means of the same experimental apparatus.

The equations of motion in antisymmetric system of two degrees of freedom are expressed by the following equations

$$-L_\beta\cdot\beta+A\ddot{\phi}-L_p\dot{\phi}-E\ddot{\psi}-L_r\dot{\psi}=L(t) \tag{24}$$

$$-N_\beta\cdot\beta-E\ddot{\phi}-N_p\dot{\phi}+C\ddot{\psi}-N_r\dot{\psi}=N(t)\,. \tag{25}$$

In the first place, in the case of the rolling system, the model is supported to rotate freely about x-axis only, as shown in Fig. 2, hence

$$\beta=\dot{\psi}=\ddot{\psi}=0 \qquad E\approx 0$$

therefore, using Eq. (25),

$$-N_p\cdot\dot{\phi}=N(t)\,. \tag{26}$$

During the forced oscillation, the model oscillates steadily with constant amplitude of the rolling angle. Therefore, it can be expressed as follows:

$$\phi=\phi_0\sin\omega t \tag{27}$$

hence

$$\dot{\phi}=\phi_0\cdot\omega\cdot\cos\omega t \tag{28}$$

where ϕ_0 is constant. Therefore, if the amplitude of the yawing moment $N(t)$ is expressed as N_0, N_p may be determined as follows:

$$N_p=-N_0/\phi_0\omega\,. \tag{29}$$

Hence, if the yawing moment $N(t)$ is measured during the rolling oscillation of the model, N_p can be determined from Eq. (29). Since the yawing moment $N(t)$ corresponds to the torsional moment about z-axis of the model, it is possible to measure it by use of a suitable pick-up.

In the same manner as in the above mentioned rolling system, in the case of the yawing system shown in Fig. 3

$$\phi=\dot{\phi}=0 \qquad \beta=-\psi$$

hence, using Eq. (24),

$$-L_\psi\cdot\psi-L_r\cdot\dot{\psi}=L(t)\,. \tag{30}$$

Since the steady yawing oscillation of constant amplitude is expressed by the following equation,

$$\psi=\psi_0\sin\omega t \tag{31}$$

substituting Eq. (31) to Eq. (30)

$$L(t) = (-L_\psi)\psi_0 \sin \omega t + (-L_r)\psi_0\omega \cos \omega t$$
$$= L_0 \sin (\omega t + \varphi_0) \tag{32}$$

where

$$L_0 = [(-L_\psi \cdot \psi_0)^2 + (-L_r \cdot \psi_0 \cdot \omega)^2]^{\frac{1}{2}} \tag{33}$$

$$\varphi_0 = \tan^{-1} L_\psi / L_r \cdot \omega \tag{34}$$

hence, derivatives L_r and L_ψ can be calculated from Eq. (33) and (34) as follows:

$$L_\psi = -L_\beta = \frac{-L_0 \cos \varphi_0}{\psi_0} \tag{35}$$

$$L_r = \frac{-L_0 \cdot \sin \varphi_0}{\psi_0 \omega}. \tag{36}$$

Though the rolling moment $L(t)$ contains two different effects of derivatives L_ψ (or L_β) and L_r, it is possible to determine these two derivatives separately with the measurement of amplitude L_0 and phase angle φ_0 of $L(t)$. Since the rolling moment $L(t)$ is a torsional moment about x-axis of the model, it is possible to measure it using a suitable pick-up which is inserted to the supporting c.g. position of the model.

The derivatives N_p, L_r and L_ψ are expressed by the following non-dimensional coefficient form

$$C_{np} = \frac{\partial C_n}{\partial\left(\frac{pb}{2V}\right)} = \frac{N_p}{\rho VS\left(\frac{b}{2}\right)^2} \tag{29$'$}$$

$$C_{lr} = \frac{\partial C_l}{\partial\left(\frac{rb}{2V}\right)} = \frac{L_r}{\rho VS\left(\frac{b}{2}\right)^2} \tag{35$'$}$$

$$C_{l\psi} = \frac{\partial C_l}{\partial \psi} = \frac{L_\psi}{\rho V^2 S\left(\frac{b}{2}\right)}. \tag{36$'$}$$

(3) Measurement of Heaving Derivatives.

It is a well-known fact that the study of short period mode oscillations with longitudinal stability is one of the latest important problems in stability analysis. In the case of this analysis, it is necessary to determine the heaving derivatives M_α, $M_{\dot\alpha}$, Z_α, $Z_{\dot\alpha}$, etc. which are derived from the heaving velocity w or the induced angle of attack $\alpha = w/V$ of the airplane, in addition to the previously mentioned stability derivatives $M_{\dot\theta}$ and M_θ in the pitching system. These derivatives can also be determined with application of the above mentioned experimental method.

As shown in Fig. 7, it is assumed that the center of rotation of the pitching system is removed to a point O' which is at a distance x from the design c.g.

position O, and the pitching oscillation is applied about the axis O' with anglar displacement Θ. The equation of motion in this system is expressed as follows:

$$I\ddot{\Theta}+(-M'_{\dot{\Theta}})\dot{\Theta}+(kl^2-M'_{\Theta})\Theta=M'(t) \tag{37}$$

where I represents the moment of inertia about O', and moment M' are all those about O'. Therefore, in this system the motion of the model is considered to be that of the combined pitching and heaving motions. The pitching angle θ and the heaving velocity w are expressed by the following equations

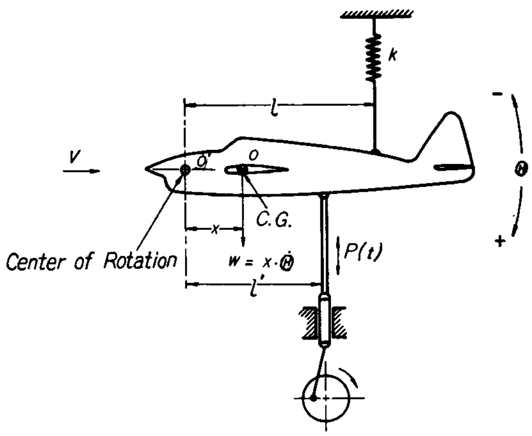

Fig. 7. Forced oscillation method. (heaving system)

$$\theta=\Theta \qquad w=x\dot{\Theta}=x\cdot\dot{\theta} \tag{38}$$

where the signs are all taken plus in the direction shown in Fig. 7. Let $M'_{\dot{\Theta}}$ and M'_{Θ} be rewritten with the aid of the stability derivatives, respectively,

$$M'_{\dot{\Theta}}=M_{\dot{\theta}}+M_{\dot{\alpha}} \tag{39}$$

$$M'_{\Theta}=M_{\theta}+M_{\alpha}+x(Z_{\theta}+Z_{\alpha}) \tag{40}$$

also

$$\alpha=w/V=x\dot{\theta}/V\,. \tag{41}$$

In the above equations $Z_{\dot{\theta}}$ and $Z_{\dot{\alpha}}$ are neglected because they are in general small quantities. Substituting Eq. (39) and (40) to Eq. (37)

$$\left(I-M_{\dot{\alpha}}\frac{x}{V}\right)\ddot{\theta}+\left(-M_{\dot{\theta}}-M_{\alpha}\frac{x}{V}-Z_{\alpha}\frac{x^2}{V}\right)\dot{\theta}$$
$$+(kl^2-M_{\theta}-Z_{\theta}\cdot x)\,\theta=M'(t)=P(t)\cdot l' \tag{42}$$

Since Eq. (42) satisfies the relation of Eq. (4), the following expressions are derived in the same way as for the previous cases.

$$2\zeta\omega_n=\frac{-M_{\dot{\theta}}-M_{\alpha}\frac{x}{V}-Z_{\alpha}\frac{x^2}{V}}{I-M_{\dot{\alpha}}\frac{x}{V}} \tag{43}$$

$$\omega_n^2=\frac{kl^2-M_{\theta}-Z_{\theta}\cdot x}{I-M_{\dot{\alpha}}\frac{x}{V}}\,. \tag{44}$$

There are six unknown stability derivatives in Eq. (43) and (44), but two relations can be derived from one value of x, as can be seen from the above equations. Therefore, it is possible to determine all the stability derivatives if three different values of x, or in other words three different centers of rotation, are chosen.

From the practical point of view, it is convenient to choose $x=0$ as one value of x, i.e. the c.g. position as one center of rotation. In Eq. (43) and (44), then $x=0$, $x=x_1$ and $x=x_2$ are chosen as the three values of x, then

$$(2\zeta\omega_n)_0 = \frac{-M_{\dot{\theta}}}{I_0} \tag{45}$$

$$(\omega_n^2)_0 = \frac{k_0 l_0^2 - M_\theta}{I_0} \tag{46}$$

$$(2\zeta\omega_n)_1 = \frac{-M_{\dot{\theta}} - M_\alpha \frac{x_1}{V} - Z_\alpha \frac{x_1^2}{V}}{I_1 - M_{\dot{\alpha}} \frac{x_1}{V}} \tag{47}$$

$$(\omega_n^2)_1 = \frac{k_1 l_1^2 - M_\theta - Z_\theta \cdot x_1}{I_1 - M_{\dot{\alpha}} \frac{x_1}{V}} \tag{48}$$

$$(2\zeta\omega_n)_2 = \frac{-M_{\dot{\theta}} - M_\alpha \frac{x_2}{V} - Z_\alpha \frac{x_2^2}{V}}{I_2 - M_{\dot{\alpha}} \frac{x_2}{V}} \tag{49}$$

$$(\omega_n^2)^2 = \frac{k_2 l_2^2 - M_\theta - Z_\theta \cdot x_2}{I_2 - M_{\dot{\alpha}} \frac{x_2}{V}} \tag{50}$$

where wind velocity V is assumed to be constant. However, since the motion in the case of $x=0$ means a pitching oscillation only about c.g. position, it is quite identical with the case of the pitching system which was mentioned in the previous section. Hence I_0 is equal to B, and $M_{\dot{\theta}}$ and M_θ are determined as follows:

$$M_{\dot{\theta}} = -B(2\zeta\omega_n)_0 \tag{51}$$

$$M_\theta = k_0 l_0^2 - B(\omega_n^2)_0 \tag{52}$$

Eq. (51) and (52) are of course identical with Eq. (19) and (20), respectively. Substituting the values of $M_{\dot{\theta}}$ and M_θ into Eq. (47), (48), (49) and (50)

$$-M_{\dot{\alpha}} \frac{x_1}{V}(2\zeta\omega_n)_1 + M_\alpha \frac{x_1}{V} + Z_\alpha \frac{x_1^2}{V} = -I_1(2\zeta\omega_n)_1 - M_{\dot{\theta}} \tag{53}$$

$$-M_{\dot{\alpha}} \frac{x_1}{V}(\omega_n^2)_1 + Z_\theta \cdot x_1 = k_1 l_1^2 - I_1(\omega_n^2)_1 - M_\theta \tag{54}$$

$$-M_{\dot{\alpha}} \frac{x_2}{V}(2\zeta\omega_n)_2 + M_\alpha \frac{x_2}{V} + Z_\alpha \frac{x_2^2}{V} = -I_2(2\zeta\omega_n)_2 - M_{\dot{\theta}} \tag{55}$$

$$-M_{\dot{\alpha}} \frac{x_2}{V}(\omega_n^2)_2 + Z_\theta \cdot x_2 = k_2 l_2^2 - I_2(\omega_n^2)_2 - M_\theta\,. \tag{56}$$

Solving the simultaneous algebraic equations (53), (54), (55) and (56), the following solutions are derived:

$$M_{\dot{\alpha}}=\frac{M_{\theta}(x_1-x_2)+\{k_1l_1^2-I_1(\omega_n^2)_1\}x_2-\{k_2l_2^2-I_2(\omega_n^2)_2\}x_1}{\frac{x_1x_2}{V}\{(\omega_n^2)_2-(\omega_n^2)_1\}} \tag{57}$$

$$Z_{\theta}=\frac{M_{\theta}\{x_1(\omega_n^2)_1-x_2(\omega_n^2)_2\}+\{k_1l_1^2-I_1(\omega_n^2)_1\}x_2(\omega_n^2)_2-\{k_2l_2^2-I_2(\omega_n^2)_2\}x_1(\omega_n^2)_1}{x_1x_2\{(\omega_n^2)_2-(\omega_n^2)_1\}} \tag{58}$$

$$Z_{\alpha}=\frac{M_{\dot{\alpha}}\frac{x_1x_2}{V}\{(2\zeta\omega_n)_1-(2\zeta\omega_n)_2\}+M_{\dot{\theta}}(x_1+x_2)-I_1x_2(2\zeta\omega_n)_1+I_2x_1(2\zeta\omega_n)_2}{\frac{x_1x_2}{V}(x_1-x_2)} \tag{59}$$

$$M_{\alpha}=\frac{M_{\dot{\alpha}}\frac{x_1x_2}{V}\{x_2(2\zeta\omega_n)_1-x_1(2\zeta\omega_n)_2\}+M_{\dot{\theta}}(x_1^2-x_2^2)-I_1x_2^2(2\zeta\omega_n)_1+I_2x_1^2(2\zeta\omega_n)_2}{\frac{x_1x_2}{V}(x_2-x_1)}\,. \tag{60}$$

Eq. (57), (58), (59) and (60) represent the stability derivatives to be determined.

Nevertheless, when numerical computation is tried in a practical case, it is found that the following relation is always satisfied in the usual wind tunnel test, even in consideration of the variable extent of x and V:

$$I \gg M_{\dot{\alpha}}\frac{x}{V}\,. \tag{61}$$

Hence, if the terms of $M_{\dot{\alpha}}$ are negligible with respect to I, the following equations are derived.

$$Z_{\theta}=\frac{-I_1(\omega_n^2)_1+k_1l_1^2-M_{\theta}}{x_1}=\frac{-I_2(\omega_n^2)_2+k_2l_2^2-M_{\theta}}{x_2} \tag{62}$$

$$Z_{\alpha}=\frac{-I_1x_2(2\zeta\omega_n)_1+I_2x_1(2\zeta\omega_n)_2+M_{\dot{\theta}}(x_1-x_2)}{\frac{x_1x_2}{V}(x_1-x_2)} \tag{63}$$

$$M_{\alpha}=\frac{-I_1x_2^2(2\zeta\omega_n)_1+I_2x_1^2(2\zeta\omega_n)_2+M_{\dot{\theta}}(x_1^2-x_2^2)}{\frac{x_1x_2}{V}(x_2-x_1)} \tag{64}$$

Eq. (62), (63) and (64) should be employed as the equations for practical calculation.

The derivatives Z_{θ}, Z_{α} and M_{α} are expressed by the following non-dimensional coefficient form

$$C_{z\theta}=\frac{\partial C_z}{\partial\theta}=\frac{2Z_{\theta}}{\rho V^2S} \tag{62'}$$

$$C_{z\alpha}=\frac{\partial C_z}{\partial\alpha}=\frac{2Z_{\alpha}}{\rho V^2S} \tag{63'}$$

$$C_{m\alpha}=\frac{\partial C_m}{\partial\alpha}=\frac{M_{\alpha}}{\rho V^2S\left(\frac{c}{2}\right)}\,. \tag{64'}$$

Because of the above mentioned reason, therefore, $M_{\dot{\alpha}}$ cannot be determined with this experimental method.

B. Experimental Apparatus and Results.

With application of the principle of measurement stated in the previous section, the experiments were tried in a low speed wind tunnel. The wind tunnel model employed in this experiment is a complete model which was constructed for use in the three components test. As an example, a schematic diagram of the experimental apparatus in the case of the pitching system is shown in Fig. 8. In the case of the rolling and yawing systems, too, they are similar to this diagram.

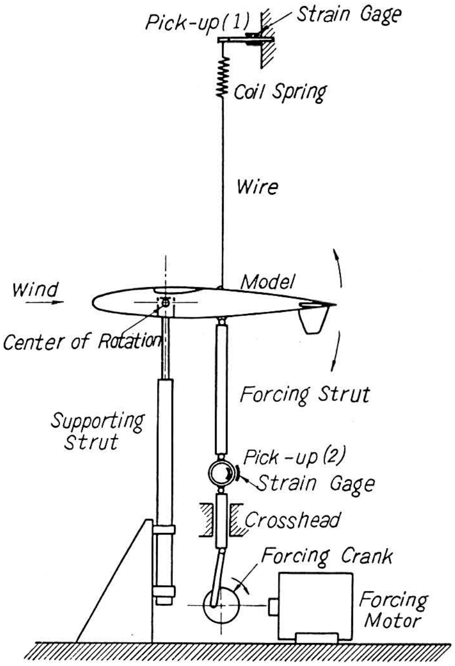

Fig. 8. Schematic diagram of forced oscillation method setup. (pitching system)

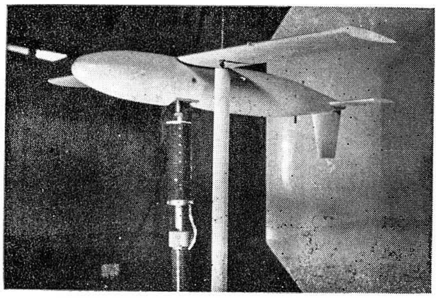

Photo 1. Model (rolling system).

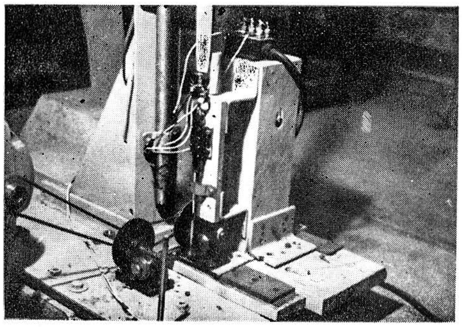

Photo 2. Forcing arrangement. Photographs in forced oscillation method.

As shown in Fig. 8, the pick-up (1) which is inserted into the supporting part of a coil spring is used to measure the system output or the pitching angle θ. The pick-up (2) which is inserted into the forcing strut of the model is similarly used to measure the applying force $P(t)$ or, accordingly, the system input moment $M(t)$. The electric transducers are all the resistance wire strain gage.

An example of the results of the experiment is shown in Fig. 9 (a), (b) and (c). Fig. 9 (a) illustrates a typical example of a recording oscillogram. In this diagram, output amplitude is always constant regardless of the forcing frequency ω. Therefore, the input amplitude a, and the phase difference between the output signal and the input signal φ should be measured in various forcing frequency ω. An example of the data in the pitching system is shown in Fig. 9 (b) and (c).

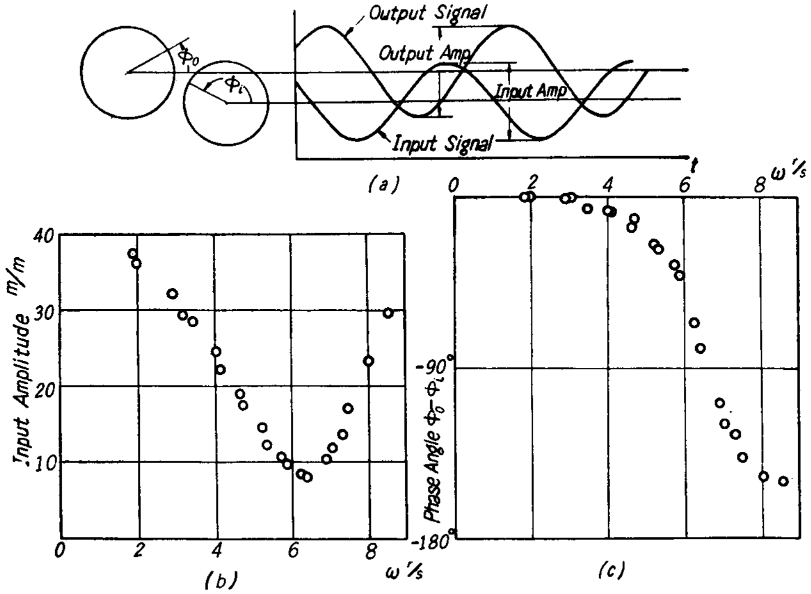

Fig. 9. Typical experimental results in forced oscillation method.

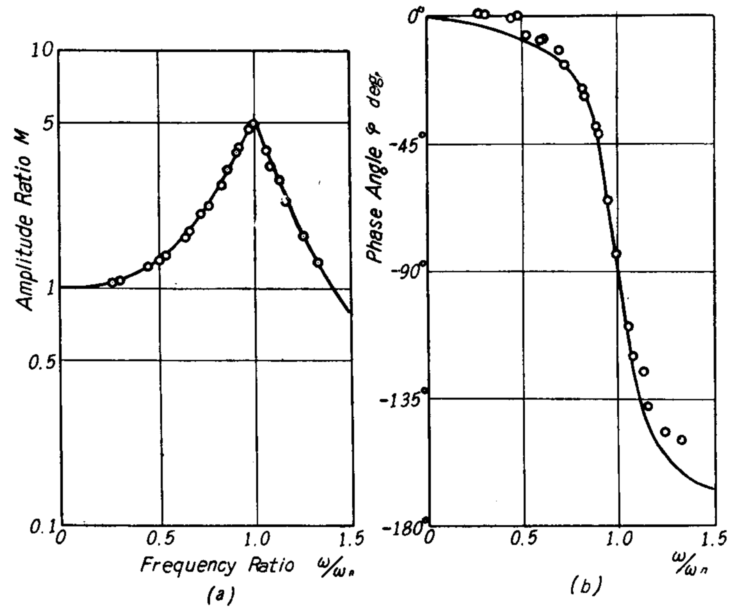

Fig. 10. Comparison of experimental results and theoretical curves. (forced oscillation method)

Table 1. Calculating table for the stability derivatives in forced oscillation method.

ω	$a_{m/m}$	$\varphi_{\text{deg.}}$	$M' = a/a_0$*	ω_n^2	$2\zeta\omega_n$	M_θ	$C_{m\theta}$	$M_{\dot\theta}$	$C_{m\dot\theta}$
5.23	16.6	−26.0	0.415	43.8	−1.48	−0.176	−0.850	−0.0100	14.62
5.76	12.5	−38.5	0.312	43.8	−1.44	−0.176	−0.850	−0.0096	14.14
5.88	12.0	−41.5	0.300	44.5	−1.50	−0.181	−0.875	−0.0101	14.70
6.25	9.3	−67.0	0.231	43.0	−1.46	−0.171	−0.825	−0.0097	14.25
6.41	9.0	−80.0	0.225	42.6	−1.47	−0.168	−0.812	−0.0098	14.35
6.90	11.8	−109.0	0.294	43.5	−1.75	−0.174	−0.840	−0.0116	17.10
7.05	12.0	−120.5	0.300	43.0	−1.58	−0.171	−0.825	−0.0105	15.43
7.35	15.5	−126.0	0.389	44.0	−1.88	−0.178	−0.860	−0.0125	18.38
7.49	17.0	−137.5	0.436	42.3	−1.67	−0.167	−0.807	−0.0111	16.32
8.05	23.2	−148.0	0.595	43.1	−1.70	−0.172	−0.831	−0.0113	16.60

Notes

$\omega = 2\pi f = \frac{2\pi}{T}$ $\quad \omega_n^2 = \omega^2/1 - M'\cos\varphi$ $\quad M_\theta = kl^2 - B(\omega_n^2)$ $\quad C_{m\theta} = \frac{M_\theta}{\rho V^2 S\left(\frac{c}{2}\right)}$

$* \, a_0 = a \Big|_{\omega=0} \cong a/\sqrt{1-\left(\frac{\omega}{\omega_n}\right)^2}$ $\quad 2\zeta\omega_n = M'\sin\varphi\cdot\frac{\omega_n^2}{\omega}$ $\quad M_{\dot\theta} = -B\cdot(2\zeta\omega_n)$ $\quad C_{m\dot\theta} = \frac{M_{\dot\theta}}{\rho VS\left(\frac{c}{2}\right)^2}$

$\omega \ll \omega_n$

These values of measurement are calculated and rearranged in Fig. 10 for comparison with the theoretical curves. Table 1 is the calculating table for estimating the stability derivatives from a result of the experiment. In this table, numerical values of the experimental data are written in the first three columns. In calculating the amplitude ratio M', i.e. the fourth column, the static input amplitude a_0 must be determined; but in practice it is convenient to estimate it by the following equation

$$a_0 = a\left\{1-\left(\frac{\omega}{\omega_n}\right)^2\right\}^{-\frac{1}{2}} \tag{65}$$

where $\omega \ll \omega_n$.

The calculations for the other columns are all presented in the previous section.

As the result of the experiment, the following phenomena were found. When the forcing moment or applying force is recorded during the forced oscillation by aid of the pickup (2), the recorded oscillating wave always contains the higher harmonics more or less, and presents a distorted wave form. It can readily be supposed that this phenomenon is due to the mechanical clearance existing in the various parts of the mechanism. Moreover, the frequency of the higher harmonics is principally determined by the rigidity of the pick-up (2). Therefore, in order to obtain accurate results of measurement, it is necessary to make the mechanical clearances in the whole mechanism as small as possible, and the rigidity of the whole mechanism containing the pick-up (2) as high as possible. Moreover, it is also necessary to insert a suitable low-pass filter between the recorder and the transducer.

Since the amplitude of the forced oscillation should be limited to the extent of no aerodynamic non-linear effect, the attitude of the model and the eccentricity of the forcing crank must be determined at the suitable values before the experiment.

In the next place, as was mentioned previously, it is also necessary to prepare other kinds of pick-ups in order to measure the cross derivatives L_r and N_p. Examples of design for these pick-ups which were employed in this experiment are shown in Fig. 11 (a) and (b). However since the magnitudes of L_r and N_p are both proportional to the lift coefficient C_L of the model, the measurement must be carried out giving the variation of angle of attack to the model.

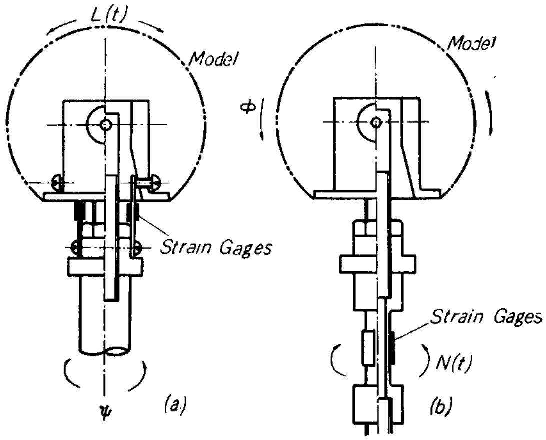

Fig. 11. Pick-ups for cross derivatives.

By means of the results of the experiment, it is found that the measurement of stiffness derivatives, i.e. M_θ and N_ψ, is relatively easy and accurate and has little relation to the forcing frequency. On the other hand, the measurement of the damping derivatives, i.e. $M_{\dot{\theta}}$, L_p and N_r, is rather difficult, especially when the damping magnitude of the system is small. Moreover, the accuracy of the measurement becomes higher when the forcing frequency is near the resonance point of the system, and lower when it is far away from it. This is due to the reason that, as can be seen from Fig. 4, Fig. 5 and Fig. 6, the effect of the damping ratio ζ is in general most remarkable near the resonance point and this inclination is more noticeable when ζ is relatively small. In other words, the above mentioned phenomenon can be understood as the frequency response characteristic of the representative second order system. Therefore, if the frequency range to be measured is decided, the mement of inertia of the model, the spring constant, the lever length, the wind velocity, etc. must all be calculated and chosen so that the measurement may be made near the particular resonance point. In the case of a weak damping system, since the accuracy of the measurement of the damping derivatives will not be so high for the above mentioned reason, the usual free oscillation method should be used in conjunction.

The measurement of cross derivatives is also not so easy, because the magnitude of the moment which is measured by the pick-ups is rather small. It is supposed that the accuracy of its measurement depends mainly upon the rigidity of the whole mechanism.

In the case of the measurement of heaving derivatives, it is necessary to choose the value of x to satisfy the oscillation condition of the system. Therefore, the value of the spring constant, the lever length, etc. must also be chosen suitably. In the same way as for the damping derivatives, the measurement should be carried out near the resonance point. Moreover, the frequency extent to be tested in this case may be decided by the characteristics of short period modes of motion. In general, it will be calculated using the condition in which the reduced frequency n is nearly equal to 0.1, where n is expressed as $\omega c/V$.

III. Transient Response Method

The forced oscillation method, as was stated in the previous section, may in general be the most excellent method for measuring stability derivatives in wind tunnels. Because, using this method, the accuracy of measurement is higher, and the calculation of experimental results is easier than for other methods, and almost all of the stability derivatives can be determined. But, for instance, in the case of closed type wind tunnels with variable pressures, or high speed tunnels, in particular of the intermittent type, it is difficult or impossible to apply this forced oscillation method.

In the case of a wind tunnel having such experimental conditions, it will therefore be convenient to determine the stability derivatives from the transient response characteristics of the model to a step control deflection. This method is an application of the experimental methods which are employed in flight test, but in the case of the wind tunnel test it will be necessary to choose the most suitable method in consideration of the differences between the flight conditions and the wind tunnel conditions.

A. Principle of Measurement.

(1) Determination by the Frequency Response Method

In the same way as for the forced oscillation method, the equations of motion in pitching, rolling and yawing systems are expressed as follows:

$$B\ddot{\theta}+(-M_{\dot{\theta}})\dot{\theta}+(kl^2-M_\theta)\theta = M_{\delta_e}\cdot\delta_e(t) \tag{66}$$

$$A\ddot{\phi}+(-L_p)\dot{\phi}+kl^2\phi = L_{\delta_a}\cdot\delta_a(t) \quad \text{or} \quad L_{\delta_r}\cdot\delta_r(t) \tag{67}$$

$$C\ddot{\psi}+(-N_r)\dot{\psi}+(kl^2-N_\psi)\psi = N_{\delta_r}\cdot\delta_r(t) \tag{68}$$

$$I\ddot{\theta}+\left(-M_{\dot{\theta}}-M_{\dot{\alpha}}\frac{x}{V}-Z_{\dot{\alpha}}\frac{x^2}{V}\right)^1\dot{\theta}+(kl^2-M_\theta-Z_\theta\cdot x)\theta = M'_{\delta_e}\cdot\delta_e(t) \tag{69}$$

where the terms $M_{\delta_e}\cdot\delta_e(t)$, $L_{\delta_a}\cdot\delta_a(t)$, $N_{\delta_r}\cdot\delta_r(t)$ etc. represent the forcing moment due to the control deflection.

Eq. (66), (67), (68) and (69) can be rewritten by the following simple equation

$$\ddot{x}+2\zeta\omega_n\dot{x}+\omega_n^2x = m_\delta\cdot\delta(t) = m_\delta\cdot\delta\cdot u(t) \tag{70}$$

for the control deflection is assumed to be a step function. Therefore, the output $x(t)$ will represent a transient response of the representative second order system to a step input. It is therefore possible to determine the coefficients of the transfer function of Eq. (70), $2\zeta\omega_n$ and ω_n^2, from this transient response data, and consequently to calculate the stability derivatives.

In the case of a step input, it is supposed that there exist various methods to determine the stabilty derivatves from the transient reponse data. But, in this paper, the subsequent determination of stability derivatives depends upon the frequency response method stated below, because this method can be compared directly with the forced oscillation method described in the previous section.

In order to obtain the frequency response from transient data, the ordinary Fourier transform is used. Since the input $\delta(t)$ is a step function in this case, as shown in Eq. (70)

$$G(s) = s\cdot X(s) = L\left\{\frac{d}{dt}x(t)\right\} = \int_0^\infty \frac{d}{dt}x(t)e^{-st}dt \tag{71}$$

therefore

$$G(j\omega) = \int_0^\infty \frac{d}{dt}x(t)e^{-j\omega t}dt\,. \tag{72}$$

If the increment of $x(t)$ between time t and $t+\Delta t$ is expressed by Δx, the frequency transfer function $G(j\omega)$ can be calculated by the following expression

$$G(j\omega) = \sum_{m=1}^{\infty} \Delta x(t_m)\ \underline{/-\omega t_m}\,. \tag{73}$$

In practice, there exists a finite time T in which $x(t)$ reaches a stationary state, as shown in Fig. 12. Therefore it is convenient to calculate $G(j\omega)$ as follows:

$$G(j\omega) = \sum_{m=1}^{n} \Delta x_m e^{-j\omega\frac{2m-1}{2}\Delta T} \tag{74}$$

$$= \sum_{m=1}^{n} \Delta x_m\left\{\cos\frac{2m-1}{2}\omega\Delta T - j\sin\frac{2m-1}{2}\omega\cdot\Delta T\right\} \tag{74$'$}$$

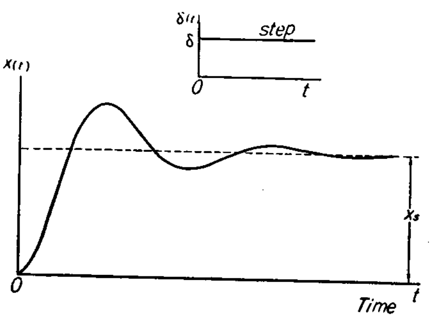

Fig. 12. Transient response to a step input in second order system.

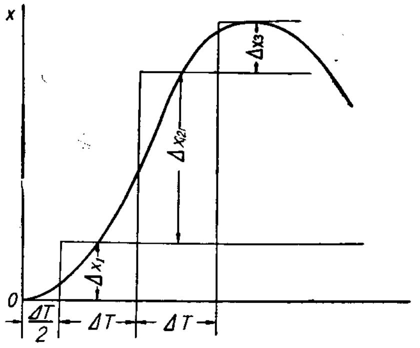

Fig. 13. Calculation of frequency response from transient data.

Eq. (74) means that the wave form of output $x(t)$ can be approximated by the total sum of step functional waves of height Δx_1, $\Delta x_2, \cdots$ etc., which are respectively shifted at uniform time intervals ΔT, as shown in Fig. 13. When $G(j\omega)$ is determined, the amplitude ratio M and the phase ange φ to any frequency ω will be determined as follows;

$$M = |G(j\omega)| = \left[\left\{1-\left(\frac{\omega}{\omega_n}\right)^2\right\}^2 + 4\zeta^2\left(\frac{\omega}{\omega_n}\right)^2\right]^{-\frac{1}{2}} \tag{75}$$

$$\varphi = \underline{/G(j\omega)} = \tan^{-1}\frac{-2\zeta\dfrac{\omega}{\omega_n}}{1-\left(\dfrac{\omega}{\omega_n}\right)^2} \tag{76}$$

Eq. (75) and (76) are quite identical with Eq. (7) and (9), respectively, in case of *the forced oscillation method*. The subsequent treatments are, therefore, entirely identical with those of the forced oscillation method in the previous section.

(2) Effect of a Initial Tangent of the Input

In the pratical calculation of frequency response, the effects of the initial tangent of the input control deflection are important subjects for study. If the control deflection is a theoretical step function

$$\delta \cdot u(t) = \lim_{T_1 \to 0} \cdot \delta(t)\,. \tag{77}$$

But in practice, it is impossible to realize the step control deflection which satisfies Eq. (77) strictly, and therefore a finite ramp time T_1 exists

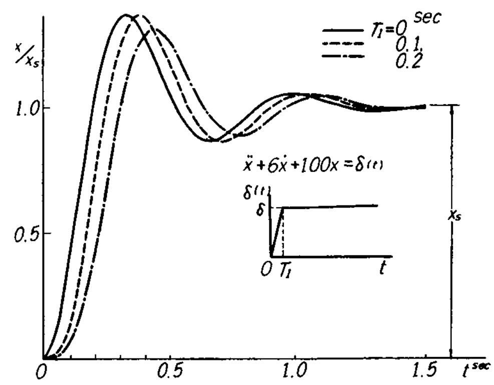

Fig. 14. Influence of ramp time T_1 in transient response curve.

inevitably (See Fig. 14.). Moreover, even if the control deflection $\delta(t)$ is a theoretical step input, it is supposed that the forcing moment $M_\delta \cdot \delta(t)$ will still be represented by the form resembling to the ramp input because of the unsteady aerodynamic effect.

Now, it is assumed that the outputs $x(t)$ for a ramp input and a step input are expressed as x_r and x_u, respectively. Let $X_U(s)$ and $X_R(s)$ denote the Laplace transform of x_u and x_r, respectively, then

$$X_U(s) = \frac{1}{\zeta^2+2\zeta\omega_n s+\omega_n^2}\cdot\frac{1}{s}\cdot m_\delta\cdot\delta \tag{78}$$

$$X_R(s) = \frac{1}{s^2+2\zeta\omega_n s+\omega_n^2}\cdot\frac{1}{s^2}\cdot\frac{m_\delta\cdot\delta}{T_1}(1-e^{-sT_1})\ . \tag{79}$$

Let $sT_1<1$, which corresponds to $\omega T_1<1$ in frequency domain,

$$e^{-sT_1} = 1-sT_1+\frac{(sT_1)^2}{2!}-\frac{(sT_1)^3}{3!}+\cdots$$

Hence

$$\frac{1-e^{-sT_1}}{sT_1} = 1-\frac{sT_1}{2!}+\frac{(sT_1)^2}{3!}-\cdots \cong e^{-\frac{T_1}{2}s}\ . \tag{80}$$

Substituting Eq. (80) to (79),

$$X_R(s) \cong \frac{1}{s^2+2\zeta\omega_n s+\omega_n^2}\cdot\frac{1}{s}\cdot m_\delta\cdot\delta\cdot e^{-\frac{T_1}{2}s}$$

$$= e^{-\frac{T_1}{2}s}\cdot X_U(s)\ . \tag{81}$$

From Eq. (81), it is found that the output $x(t)$ for a ramp input is approximately equal to the output for a step input having a time lag of $T_1/2$, if the ramp time is too small to satisfy the condition of $\omega T_1<1$.

In the treatment of the stability problems of an airplane, since the frequency of oscillating motion is at most less than 2 or 3 cycles per second in general, it will not be so difficult to satisfy the condition of $\omega T_1<1$. As an example, the results of numerical calculation in case of $\omega_n=10$ are illustrated in Fig. 14. From this diagram, it is found that the relation of Eq. (81) is fully satisfied even in the case of $T_1=0.1$ or $\omega_n T_1=1$. By means of theoretical calculation, the error in the case of $\omega_n T_1=1$ is only about 2 percent. Therefore, in experiment, a ramp input can be substituted satisfactorily for a step input if the former has the ramp time T_1 which satisfies the condition of $\omega_n T_1<1$. Moreover, it is found that the curve of $T_1=0.2$ illustrated in the same diagram expresses that the larger T_1 affects not only the time lag but also the amplitudes of the wave form.

(3) Determination of the Initial Point of the Output Curve

In the next place, it is also practical to study to determine the point of $t=0$

or the initial point of the curve of output $x(t)$. If the initial ramp time T_1 has been measured, it is reasonable to choose a point having a delay time of $T_1/2$, but if T_1 is unknown, it is convenient to utilize the following relations.

In the case of a step input, as shown in Eq. (70), since the initial condition is a stationary state, the output $x(t)$ is given as follows:

$$x(t) = x_s\left[1-e^{-\zeta\omega_n t}\cdot\frac{1}{\sqrt{1-\zeta^2}}\sin\left(\omega_n\sqrt{1-\zeta^2}\cdot x+\Phi\right)\right] \tag{82}$$

where

$$x_s = \frac{m_\delta\cdot\delta}{\omega_n^2} \tag{83}$$

$$\Phi = \tan^{-1}\frac{\sqrt{1-\zeta^2}}{\zeta} \tag{84}$$

x_s is a constsant value corresponding to the equilibrium condition of output x against the control deflection δ. Therefore, as shown in Fig. 15, since $x(t)$ expresses a damped oscillation in which x_s is the mean value, the initial curve of the output to a step input is considered to be a part of the curve of phase lead Φ, as shown in Eq. (82). Since Φ is a function of the damping ratio ζ only as shown in Eq. (84), it is covenient to choose $t=0$ as a time about a quarter period before the crossing point between the initial wave and the straight line $x=x_s$, when ζ is relatively small.

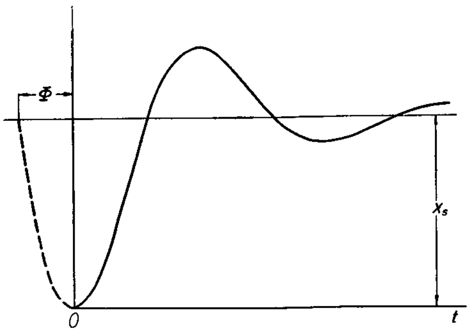

ζ	Φ	ζ	Φ
0	90°	0.3	72.5°
0.1	84.3°	0.4	66.4°
0.2	78.5°	0.5	60.0°

Fig. 15. Phase lead Φ for a step input.

In the case of the transient response method, it is therefore impossible to determine the stability derivatives $M_{\dot{\alpha}}$, L_r, L_ψ and N_p.

B. Experimental Apparatus and Results

As has been stated previously, the transient response method is particularly suitable for a high speed wind tunnel test. But, because of the experimental equipment, the following preliminary experiment with application of this method was made in a low speed wind tunnel. The wind tunnel and the model which were employed in this experiment are therefore entirely the same as those in the case of the forced oscillation method. The experiment was made with a pitching system. The schematic diagram of the experimental apparatus is shown in Fig. 16. The mechanism giving a step deflection to the elevators in this example is shown in Fig. 17, which is the setup combining a electromagnet and a coil spring. A magnitude of the elevator deflection δ_e must be chosen so that the attitude of the model is limited in the extent to which the slope of lift and the pitching moment against the angle of attack is linear. In practice, the numerical value of δ_e was about 5 degrees.

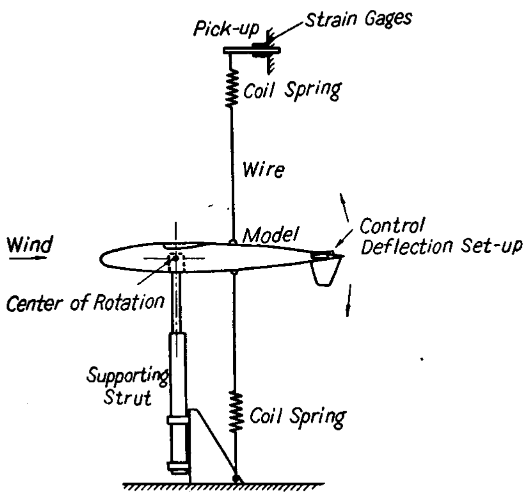

Fig. 16. Schematic diagram of transient response method setup. (pitching system)

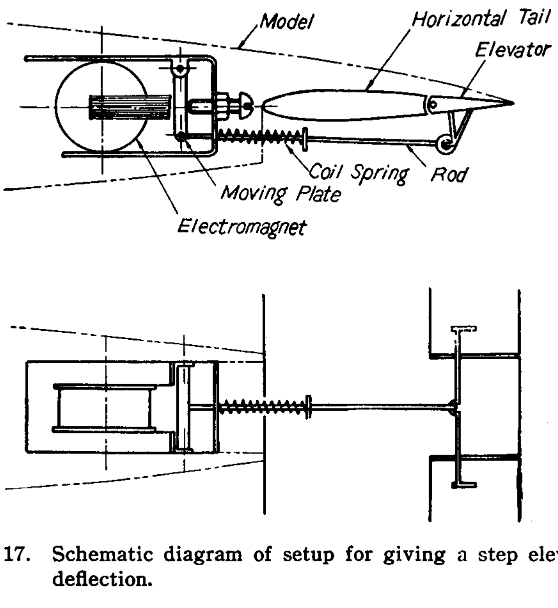

Fig. 17. Schematic diagram of setup for giving a step elevator deflection.

The detector of the output, or the pitching angle θ in this system, is the pick-up which was inserted into the supporting part of the spring, in the same way as for the forced oscillation method. The electric transducer is the wire strain gage in this case also.

The amplitude ratio M and the phase angle φ which has been calculated from a recorded output curve are respresented in Fig. 18 (a) and (b). Moreover, the numerical values of the stability derivatives which have been calculated from the above mentioned data are shown in Table 2. From these experimental results too, it is obvious that the data far removed from the resonance point in frequency are useless for practical purposes because of their low accuracies. The reason for this phenomenon is the frequency response characteristics of a second order system as has been stated in detail in the case of the forced oscillation method. In order to determine the accurate values of stability derivatives, it is therefore necessary to choose frequency ω in more instances near to the natural frequency ω_n particularly.

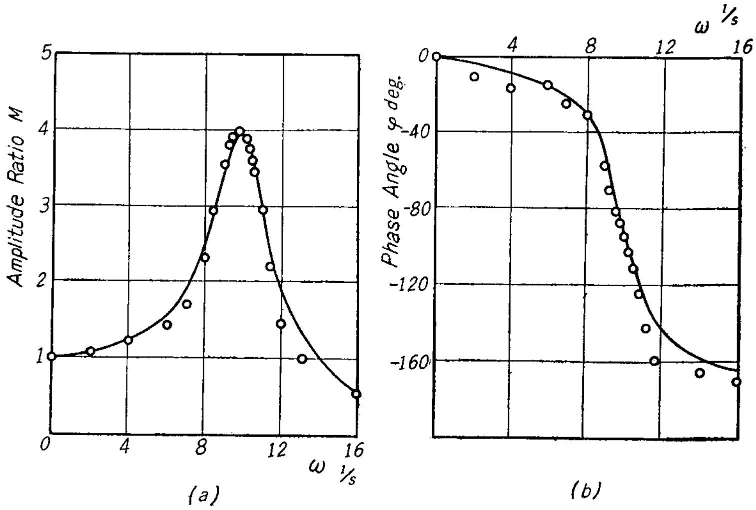

Fig. 18. Comparison of experimental results and theoretical curves. (transient response method)

Table 2. Experimental results in transient response method.

ω	$2\zeta\omega_n$	ω_n^2	$C_{m\theta}$	$C_{m\theta}$
8.5	2.50	98.0	−0.883	−19.7
9.0	2.53	96.0	−0.865	−20.0
9.4	2.52	95.8	−0.863	−19.9
9.6	2.50	95.8	−0.863	−19.7
9.8	2.46	96.0	−0.865	−19.4
10.0	2.42	96.0	−0.865	−19.0
10.2	2.32	96.1	−0.866	−18.25
10.4	2.21	96.1	−0.866	−17.35
10.6	2.07	96.0	−0.865	−16.1

In comparison with the values obtained using the forced oscillation method, which are shown in Table 1, the measurement by the transient response method may be considered to have sufficiently high accuracies.

IV. Concluding Remarks

As experimental methods for determining the stability derivatives of an airplane employing the wind tunnel model, the forced oscillation method with constant amplitude and the transient response method have been represented. The principles of measurement are, in both cases, those calculating the stability derivatives from the frequency response characteristics of a second order system. Therefore, in the case of the large damping ratio of the system, the measurements are easier and more accurate. When the damping ratio is too small, it will therefore be convenient to apply these methods together with the ordinary free oscillation method.

Moreover, the forced oscillation method described above is applicable to the measurement of negative damping systems and aerodynamic unsteady effects in case of high frequency.

Acknowledgement

The author expresses hearty thanks to Mr. T. Shibata, H. Nakai, I. Ogawa and N. Nakayama for their kind assistance in carrying out the experiments and the numerical calculations.

The author adds here that the present report is a summarized result of research performed under a Science Research Grant of the Ministry of Education.

Nomenclature

A	: moment of inertia about	x-axis
B	: 〃	y-axis
C	: 〃	z-axis
E	: product of inertia	
$G(s)$	: transfer function	
K	: static gain	
$L(t)$	: rolling moment	
M	: amplitude ratio	
$M(t)$	: pitching moment	
$N(t)$	: yawing moment	
$P(t)$	: applied force	

S	:	wing area	
V	:	wind velocity	
b	:	wing span	
c	:	m.a.c.	
k	:	spring constant	
p	:	rolling angular velocity	
q	:	pitching "	
r	:	yawing "	
$u(t)$	:	unit step function	
w	:	heaving velocity	
α	:	angle of attack	
β	:	sideslip angle	
δ	:	control deflection	
δ_a	:	aileron angle	
δ_e	:	elevator angle	
δ_r	:	rudder angle	
ζ	:	damping ratio	
θ	:	pitching angle	
ρ	:	air density	
ϕ	:	rolling angle	
φ, Φ	:	phase angle	
ψ	:	yawing angle	
ω	:	circular frequency	
M_θ	:	stability derivative	$\partial M/\partial\theta$
M_α	:	"	$\partial M/\partial\alpha$
$M_{\dot{\alpha}}$	:	"	$\partial M/\partial\dot{\alpha}$
M_q	:	"	$\partial M/\partial q$
L_p	:	"	$\partial L/\partial p$
$L_\psi=-L_\beta$	:	"	$\partial L/\partial\psi=-\partial L/\partial\beta$
N_r	:	"	$\partial N/\partial r$
$N_\psi=-N_\beta$	:	"	$\partial N/\partial\psi=-\partial N/\partial\beta$
L_r	:	"	$\partial L/\partial r$
N_p	:	"	$\partial N/\partial p$
Z_θ	:	"	$\partial Z/\partial\theta$
Z_α	:	"	$\partial Z/\partial\alpha$
M_{δ_e}	:	control effectiveness	$\partial M/\partial\delta_e$
L_{δ_a}	:	"	$\partial L/\partial\delta_a$
N_{δ_r}	:	"	$\partial N/\partial\delta_r$

References

1) W. J. Duncan; "Control and Stability of Aircraft" Cambridge Press, (1952)
2) C. D. Perkins and R. E. Hage; "Airplane Performance, Stability and Control" John Wiley & Sons, (1954)
3) B. Etkin; "Dynamics of Flight" John Wiley & Sons, (1959)
4) J. Valensi; AGARD (1954)
5) S. Uehara; Jour. JSAS, 7, 209 (1959)
6) S. Neumark and A. W. Thorpe; R & M No. 2902 (1955)
7) C. Scruton, L. Woodgate and A. J. Alexander; R & M No. 2925 (1957)
8) G. F. Moss; R & M No. 3009 (1957)
9) M. E. La verne and A. S. Boksenbom; NACA TR No. 977 (1950)
10) H. J. Curfman and R. E. Gardiner; NACA TR No. 984 (1950)
11) J. J. Donegan and H. A. Pearson; NACA TR No. 1070 (1952)
12) J. M. Eggleston and C. W. Mathews; NACA TR No. 1204 (1954)
13) W. C. Triplett, S. C. Brown and G. A. Smith; NACA TR No. 1250 (1955)